

# Wear Behavior of Iron Based Alloys with Different Entropy Extent Estimated by Miedema's Model

Asaad Kadhim Eqal<sup>a\*</sup> , Haidar Akram Hussein<sup>b</sup> 

<sup>a</sup>Southern Technical University, Amarah Technical Institute, 44001, Amarah, Iraq.

<sup>b</sup>Middle Technical University, Technical Engineering College, 10074 Baghdad, Iraq.

Received: July 28, 2023; Revised: November 21, 2023; Accepted: January 05, 2024

In most situations, predicting wear requires a variety of microstructural characterizations and experiments with contact surfaces. Based on physical principles, mathematical models might be of great assistance in understanding and thereby predicting this event. Considering the significance of heat generation in wear, it appears that the parameters of thermodynamics are appropriate measurements for wear modelling. Entropy is among these parameters of thermodynamics. The Miedema model is a good method to predict the Gibbs free energy and entropy of solid solutions of binary and ternary systems. In this study, the wear behaviour of iron-based alloys according to their estimating values of Gibbs free energies and entropy was studied under lubricated conditions. The wear test was performed in accordance with ASTM-G99, utilizing the vertical universal friction testing machine MMW-1A and the pin-on-disk test methodology. Results show that the lowest negative value of Gibbs free energy was noted in the Fe-Al-Sn ternary system (-14.37 KJ/mol), while the highest negative value was found in the Fe-Al-V (-25.16 KJ/mol) binary system. It was also concluded that the wear rate decreased when the entropy estimate increased. The higher value of the wear rate was ( $6.935 \text{ mm}^3/\text{N.m} \times 10^7$ ) for Fe-Al binary alloy with an entropy value (1.717 J/k Mole). The lowest value of wear rate was ( $3.581 \text{ mm}^3/\text{N.m} \times 10^7$ ) for Fe-Al-Sn ternary alloy with an entropy of (2.71 J/k Mole). This is due to the micro-distortion that was mechanically indicated with the ternary alloys Fe-Al with V, Mn, Ga, B, and Sn additives that affected the wear mechanism and caused high values of wear.

**Keywords:** Friction, lubricant, enthalpy, Gibbs free energy, severe lattice distortion.

## 1. Introduction

The appreciable improvement in mechanical properties of alloys is due to the chemical and structural disorder present in the high entropy phase. These include high configurational entropy and severe lattice distortion<sup>1</sup>. Entropy can be used as a basic method for quantifying degradation, including wear and friction. This is due to the fact that entropy is a thermodynamic notion, so using the laws of thermodynamics and heat transport will be essential<sup>2</sup>. Therefore, high-entropy alloys (HEAs) offer numerous unique and exceptional features that distinguish them from normal alloys, including superior high-temperature oxidation resistance, mechanical properties, corrosion resistance, and friction resistance<sup>3,4</sup>. Previously, it was thought that alloys containing multiple principles would result in a complex phase composition and subpar performance, so these alloys were not desired. Nevertheless, much research on alloys containing multiple principles has shown that high-entropy alloys are achievable with a single phase (BCC or FCC). In addition, these alloys offer several advantages over existing alloys, such as significant improvements in strength, oxidation resistance, corrosion resistance, ductility, and thermal stability<sup>5</sup>. The intermetallic compounds of Fe-Al based alloys have long been regarded as interesting choices in producing structural materials utilized in high-temperature settings. Adding a specific quantity of a third element, such as boron, to alloys is well known to significantly increase their mechanical characteristics<sup>6-8</sup>.

Additionally, the Fe-Al alloys, together with Ga or B, can elucidate the connection among mechanical, physical, and tribological properties. These alloys are recognized as being inexpensive and can be synthesized. The diagrams of the phase state of binary systems have been extensively considered and found to be highly reliable<sup>9,10</sup>. The ternary systems diagrams (e.g., those Fe-Al based alloys) are more inclined to be researched than other alloys<sup>11,12</sup>. The methods adopted for evaluating the enthalpy frequently include CALPHAD, the Miedema model, and others. These methods are used to calculate the equilibrium diagrams using Gibbs energy as an important parameter of the model<sup>13</sup>. In this regard, various suggested modified Miedema models have provided the most reasonable results<sup>14,15</sup>. It is necessary to argue that the CALPHAD approach is widely applied in predicting the thermodynamic properties and phase diagrams, which are based on the extrapolation and optimization of several experimental findings of thermodynamic properties and phase equilibrium. The relationship between the entropy generated (dissipated energy) and wear has been demonstrated by many studies that have been done to predict wear using an energy basis. Jahangiri et al.<sup>16</sup> Examined a mathematical model and produced an entropy rate for sliding wear of AISI 4140 SS and a 70–30 brass contact pair. For both irreversible and reversible processes, the generated entropy rate relationship may be derived. From the result, the temperature of 70–30 brass showed a linear relationship between its rate of wear and the generated entropy. Nosonovsky et al.<sup>17</sup>

\*e-mail: [asaad.kadhim@stu.edu.iq](mailto:asaad.kadhim@stu.edu.iq)

Reviewed the application of entropy to wear and friction, which employ the entropic thermodynamic technique in addition to applying the entropy notion mathematically to the dynamic friction effects and perhaps establishing a link between the information and thermodynamic approaches. Lijesh et al.<sup>18</sup> Investigated the multiple wear rates using the degradation entropy generation theory, a thermodynamically based method. A streamlined process that considers the existence of many wear regimes is suggested, utilizing the DEG theory, degradation coefficient, and friction coefficient values for each wear mode. The major aim of this work is to examine the wear behaviour with regard to the Gibbs free energy and entropy estimated by using the Miedema model of solid solution of binary and ternary systems of iron-based alloys Fe-Al with V, Mn, Ga, B, and Sn additives.

## 2. Theoretical Study

### 2.1. Miedema's Model

One method for estimating the thermodynamic variables of a solid solution is the Miedema model. The creation enthalpy of both liquid and hard alloys can be directly computed using the Miedema model (semi-empirical)<sup>13,19,20</sup>. Two variables influence an alloy's mixing enthalpy. The two components have an electronegativity variation ( $\Delta\phi^*$ ) and an electron density differential ( $\Delta n_{ws}^{1/3}$ ). When considering their contributions to the mixing enthalpy, they are diametrically opposed, with the first one having a contribution that is classified as negative. In contrast, the other has a reverse contribution<sup>21,22</sup>. The Miedema model may be used to write the formula for enthalpy production ( $\Delta H$ ) in a binary system<sup>19,22</sup>.

$$:\Delta H = C_A f_B^A S(c) \Delta H_{A \text{ in } B}^{\text{interface}} \quad (1)$$

$$\Delta H_{A \text{ in } B}^{\text{interface}} = \frac{V_A^{2/3}}{\left(\frac{1}{n_{ws}^3}\right)_{av}} P \left[ -(\Delta\phi^*)^2 + \frac{Q}{P} \left( \Delta n_{ws}^{1/3} \right)^2 - \frac{R}{P} \right] \quad (2)$$

$$f_B^A = C_B^S \left[ 1 + 8 \left( C_A^S C_B^S \right)^2 \right] \quad (3)$$

$$C_A^S = \frac{C_A V_A^{2/3}}{C_A V_A^{2/3} + C_B V_B^{2/3}} \quad (4)$$

$$C_B^S = \frac{C_B V_B^{2/3}}{C_A V_A^{2/3} + C_B V_B^{2/3}} \quad (5)$$

$$S(c) = 1 - \frac{C_A^S |V_A^{2/3} - V_B^{2/3}|}{C_A^S V_A^{2/3} + C_B^S V_B^{2/3}} \quad (6)$$

Where the multiplicative factor  $f_B^A$  accounts for the elemental surface concentration, The heat of solid solution formation A in B, kJ/mol is represented by  $\Delta H_{A \text{ in } B}^{\text{interface}}$ ; A prefactor known as S(c) is added when the forms of the contact cells between two substances alter; the concentrations of

elements A and B, expressed in  $\text{cm}^{-3}$  are  $C_A, C_B$ ; The molar volumes of the components A, B, in  $\text{cm}^3/\text{mol}$  are  $V_A, V_B$ ; The Wigner-Seitz cell boundary's electron density is represented by  $n_{ws}$ ; V, P, Q/P, R/P are constants;  $\phi^*$  - electronic chemical potential, The elements A and B have surface concentrations represented by the  $C_A^S, C_B^S$ .

### 2.2. Gibbs Free Energy ( $\Delta G$ ) Calculations

Using the following formula, the Gibbs free energy can be found for crystalline solid solutions A and B:

$$\Delta G_{ss} = \Delta H_{ss} + T \Delta S_{ss} \quad (7)$$

Where  $\Delta H_{ss}$  and  $\Delta S_{ss}$  refer to the mixing enthalpy change and mixing entropy change of solid solutions, respectively, and T refer to the temperature at which a solid solution forms, which is its absolute temperature. When entropy is the sole factor taken into account, Eq. 11 may be used to compute the mixing entropy change of a solid solution:

$$\Delta S_{ss} = \Delta S_C \quad (8)$$

Where configurational entropy is denoted by  $\Delta S_C$ .

## 3. Material Used

Iron-based alloys, Fe-Al, Fe-Al-Mn, Fe-Al-V, Fe-Al-Ga, Fe-Al-B, and Fe-Al-Sn, were tested for their wear resistance at room temperature. A wear test was conducted using the vertical universal friction and wear testing machine (MMW-1A), as shown in Figure 1. The machine standard was according to the ASTM G-99 pin-on-disc test principle. The device was counted using the three-pin, single-disc method.

### 3.1. Sample Preparation

As the starting materials for the mechanical synthesis, powdered elements that are pure, such as iron (of 99.5% purity), aluminium (of 99.99% purity), tin (of 99% purity), boron (of 99% purity), gallium (of 99% purity), manganese (of 99.5% purity), and ferrovanadium (Fe60V40), were used. Powders with a particle size between (+75  $\mu\text{m}$ ) and (-300  $\mu\text{m}$ ) were utilized. Powder mixtures of Fe (65% white) and Al (35% white) were used to create a binary alloy, while powder mixtures of Fe and Al with one of these elements were used to create a ternary alloy. The components of the alloy were added in weight proportions that matched predetermined concentrations. A planetary ball mill was used for mechanical alloying in an argon environment. This was used in the current investigation to determine the time and conditions of mechanical synthesis. A mechanical milling period of 16 hours is adequate to make single-phase homogenous iron alloys<sup>23</sup>. The Fe-Al binary alloy containing (4.5-5) weight percent of each of the additional elements (V, Mn, Ga, B, and Sn) was obtained after mechanical synthesis. These materials were vacuum annealed to a temperature between (500 and 800 °C) using an induction furnace, followed by water quenching<sup>24</sup>. The pin-on-disc test standard was followed in the preparation of the samples. After the samples were ground using SiC sheets with varying grain sizes, a suspension of 0.3-micrometer alumina was employed for polishing. The samples were cleaned with water, then alcohol, and finally air-dried.



**Figure 1.** Vertical universal friction testing machine (MMW-LA), samples and samples fixture.

The dimensions of the cylindrical shape of the pin are (6 mm in diameter and 16 mm in height), while the inner and outer diameters of the disk (16mm and 32mm) respectively, with an (11mm) thickness. The pin's metal is an iron-based alloy, and the ring is (CK50). The test was carried out at constant sliding speed (500 rpm), constant load (100 N), constant time (30 min), and constant sliding distance (900 m) at room temperature.

### 3.2. Lubricant

Moulding oil, used especially in die manufacturing, was selected as mineral oil. Properties are tabulated in Table 1.

## 4. Results and Discussion

Figure 2 shows the X-ray diffraction for Fe-Al alloying, in which only the system of BCC was presented in the pattern of X-ray diffraction of all the components. The diffractometer uses  $\text{Cu K}\alpha$  ( $\lambda=1.5418 \text{ \AA}$ ) radiation scanning between  $20^\circ$  to  $120^\circ$  with a scanning rate of  $1^\circ/\text{s}$ . The compositional structure was analyzed by X-ray diffraction using diffractometers DRON-3M and SMARTLAB (Rigaku), a Ni monochromator and  $\text{CuK}\alpha$  radiation at room temperature.

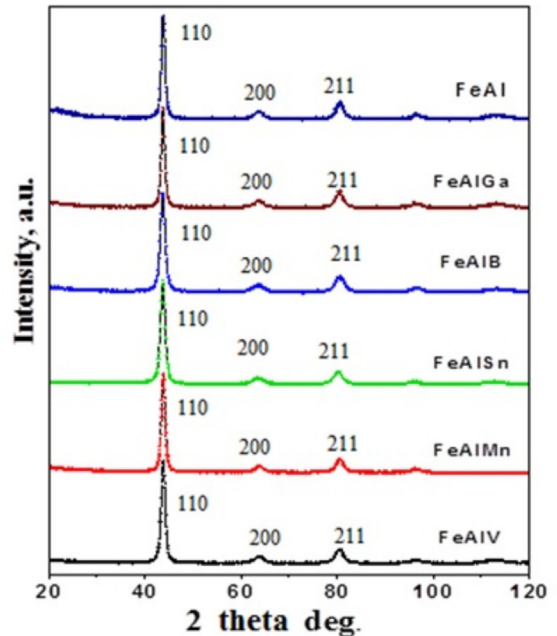


**Figure 2.** X-ray diffraction patterns.

**Table 1.** The properties of mineral oil that used to lubricant.

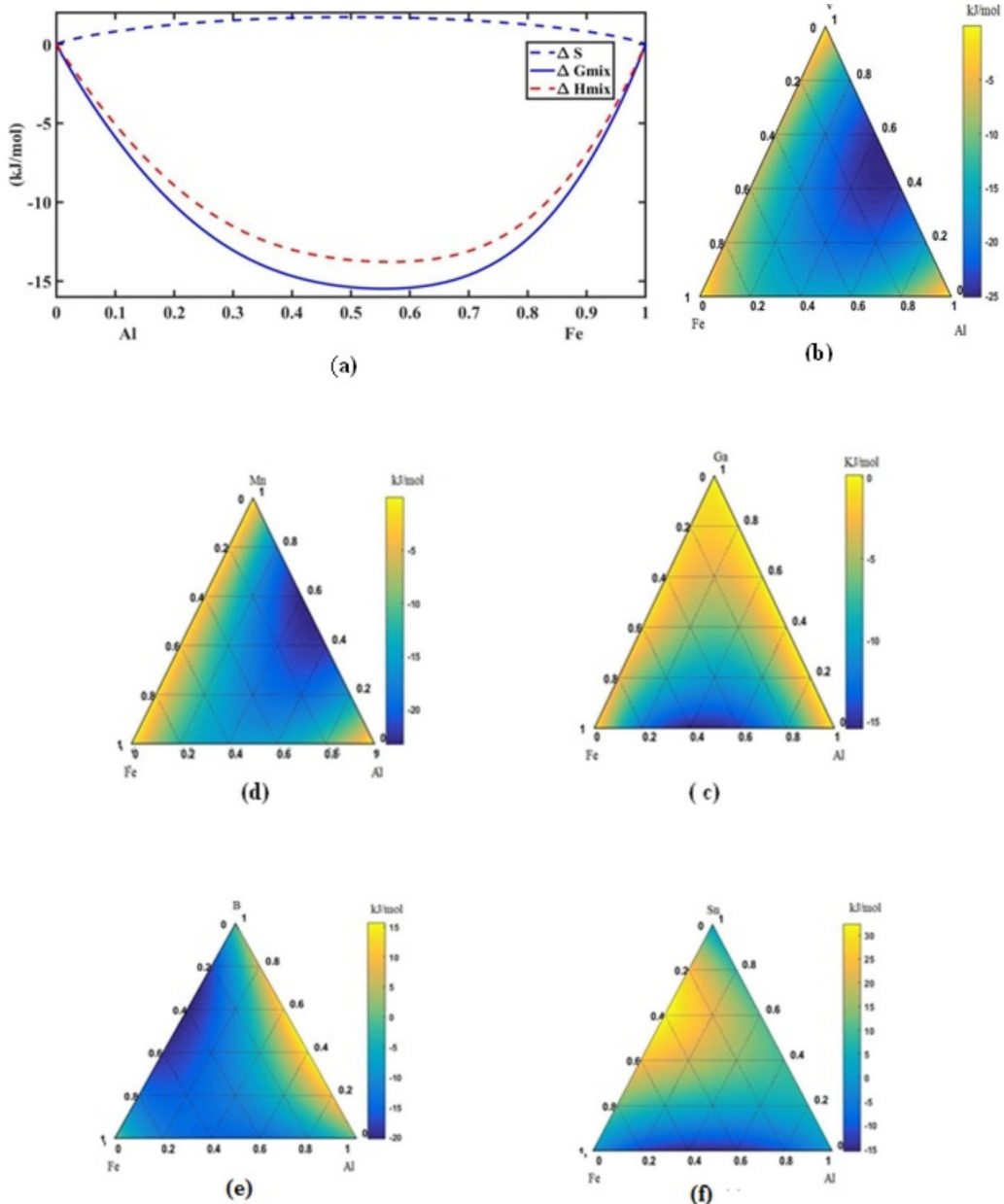
Laboratory temperature Data	Kinematic Viscosity $\text{mm}^2/\text{s}$ 40 $^\circ\text{C}$	Kinematic Viscosity $\text{mm}^2/\text{s}$ 100 $^\circ\text{C}$	Viscosity Index	Specific Gravity at 15.6 $^\circ\text{C}$	COC* flash point $^\circ\text{C}$	Pour Point $^\circ\text{C}$
Moulding	15.37	3.61	119	0.858	190	-9

\*COC Cleveland Open Cup test: All values are critical specifications defined by ASTM D 3244. To ensure full lubrication in the contact zone and full oil circulation, pour oil into the container until the oil level fills about 7 to 9 mm from the sliding ring's edge.

This implies Al and additional atoms dissolve in iron, producing the BCC solid solution of  $\alpha$ -Fe (Al). In accordance with the results of the X-ray examination, the ternary alloys Fe-Al, including V, Mn, Ga, B, and Sn, that were created using mechanical alloying techniques were single-phase materials with a significant amount of micro-distortion.

The Gibbs free energy ( $\Delta G$ ) of mixing binary and ternary solid solution was computed and plotted as shown in Figure 3. It is possible to notice the negative values of Fe-Al, Fe-Al-V, Fe-Al-B, Fe-Al-Mn, Fe-Al-Ga, and Fe-Al-Sn. The values of Gibbs free energy ( $\Delta G$ ) of the solid solution alloys were recorded as (-15.48 KJ/mol,

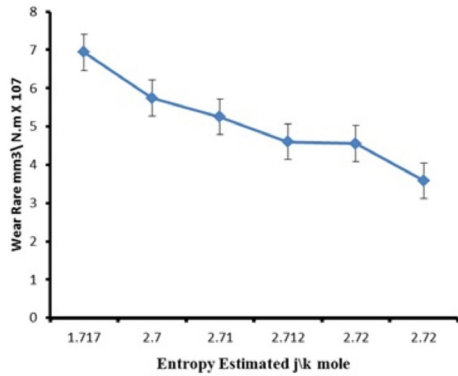
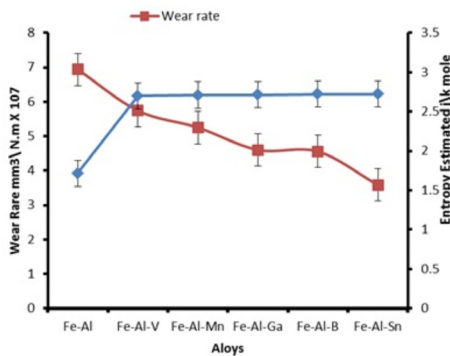
-25.16 KJ/mol, -23.3 KJ/mol, -15.22 KJ/mol, -20.03 KJ/mol and -14.37 KJ/mol) as shown in Figure 3a, b, c, d, e, and f respectively. Based on thermodynamics, a system seeks to reduce its Gibbs free energy ( $G$ ) in isothermal and isobaric conditions. Accordingly, equilibrium is achievable upon the Gibbs energy reaching its minimal state. This, in turn, means a thermodynamic force allowed a binary system to release its stored energy to create these phases<sup>12</sup>. The highest negative value of Gibbs free energy was noted in the Fe-Al-V ternary system (-25.16 KJ/mol), while the lowest negative value was found in the Fe-Al-Sn (-14.37 KJ/mol) binary system.



**Figure 3.** Gibbs free energy of mixing as a function of composition of the binary and ternary system, of (a) Fe-Al, (b) Fe-Al-V, (c) Fe-Al-Mn, (d) Fe-Al-Ga, (e) Fe-Al-B, and (f) Fe-Al-Sn.

**Table 2.** The relationship between Entropy estimated and Gibbs free energy and type of alloys.

Alloy	Entropy Estimated J/k Mole	Gibbs Free Energy KJ/mol
Fe-Al	1.717	-15.48
Fe-Al-V	2.72	-25.16
Fe-Al-Mn	2.7	-23.3
Fe-Al-Ga	2.712	-15.22
Fe-Al-B	2.72	-20.03
Fe-Al-Sn	2.71	-14.37

**Figure 4.** The wear rate versus Entropy estimated of alloys.**Figure 5.** The relationship between the wear rate and Entropy estimated with type of alloys.

The result shows that the estimating values of the entropy ( $\Delta S$ ) for binary and ternary systems reveal that the minimum value of the entropy ( $\Delta S$ ) was related to the Fe-Al alloys compared to the other alloys as shown in Table 2. It is noticeable that the value of entropy for the Fe-Al was the lowest value (1.717 J/k Mole) compared with the Fe-Al-V (2.72 J/k Mole), Fe-Al-Mn (2.7 J/k Mole), Fe-Al-Ga (2.712 J/k Mole), Fe-Al-B (2.72 J/k Mole), and Fe-Al-Sn (2.71 J/k Mole). The metallurgical characteristics lead to an expected increase in entropy with varying alloys. This is because of the significant solution hardening that results from the severely distorted lattice. The effects of high entropy can lead to simple

solid solutions instead of intermetallic compounds. The severe lattice distortion can influence mechanical, chemical, and physical properties slow diffusion can encourage the development of amorphous structures, or noncrystalline and cocktail effects can result in novel properties owing to the interaction of elements<sup>25-27</sup>. The entropy results from this analysis differ from those from prior studies<sup>16,18</sup>. This is because these studies obtained generated entropy from the friction of two surfaces, whereas, in the current study, the entropy estimated by using the Miedema model.

Previous studies<sup>16-19</sup> have also reported a linear relationship between the generated entropy and wear rate. Nonetheless, a more basic mathematical approach has been used in the present study to elucidate the rationale for using entropy: an accurate differential. When the entropy ( $\Delta S$ ) of the binary and ternary increases, the wear rate decreases in semi-linear relations, as shown in Figure 4. This is related to the dissipative processes' entropies, which serve as influence functions on the wear mechanism. The increased interfacial energy in the system focuses on the interfacial boundaries between the substrate and additives, which forms the foundation of the proposed mechanism of action of the additive. The large degree of micro-distortion that mechanically indicated with the ternary alloys Fe-Al with V, Mn, Ga, B, and Sn affected the wear mechanism, causing high values of wear, as shown in Figure 5.

## 5. Conclusions

The conclusions of this study indicated that the Gibbs free energy and entropy of a solid solution for binary and ternary systems can be predicted using the Miedema model. The results showed that the highest negative value of Gibbs free energy was noted in the Fe-Al-V ternary system because it seeks to reduce its Gibbs free energy ( $G$ ), according to thermodynamics, to reach equilibrium. It is evident that the value of entropy for Fe-Al was the lowest value (1.717 J/k Mole) compared with the Fe-Al-V (2.72 J/k Mole), Fe-Al-Mn (2.7 J/k Mole), Fe-Al-Ga (2.712 J/k Mole), Fe-Al-B (2.72 J/k Mole), and Fe-Al-Sn (2.71 J/k Mole). This is because the additive's proposed mode of action is based on the enhanced interfacial energy in the system, which is concentrated at the interfacial boundaries between the substrate and additives. Also concluded was that the wear rate decreased when the entropy estimated increased for a ternary system, solid solution. This is due to the micro-distortion that mechanically indicated with the ternary alloys Fe-Al with V, Mn, Ga, B, and Sn affected the wear mechanism with high values of wear.

## References

1. Feltrin AC, Xing Q, Akinwekomi AD, Waseem OA, Akhtar F. Review of novel high-entropy protective materials: wear, irradiation, and erosion resistance properties. *Entropy*. 2022;25(1):73. <http://dx.doi.org/10.3390/e25010073>.
2. Amiri M, Modarres M. An entropy-based damage characterization. *Entropy*. 2014;16(12):6434-63. <http://dx.doi.org/10.3390/e16126434>.
3. Liang ML, Wang CL, Liang CJ, Xie YG, Liu WJ, Yang JJ, et al. Microstructure and sliding wear behavior of FeCoNiCr<sub>0.8</sub>Al<sub>0.2</sub> high-entropy alloy for different durations. *Int J Refract Hard Met*. 2022;103:105767. <http://dx.doi.org/10.1016/j.ijrmhm.2021.105767>.
4. Yang J, Wang C, Xie D, Qin H, Liu W, Liang M, et al. A new type of gradient structure FeCoCrNiWMo high entropy alloy layer by plasma solid-state surface metallurgy. *Surf Coat Tech*. 2023;457:129320. <http://dx.doi.org/10.1016/j.surfcoat.2023.129320>.
5. Liu Y, Zhang F, Huang Z, Zhou Q, Ren Y, Du Y, et al. Mechanical and dry sliding tribological properties of CoCrNiNb<sub>x</sub> medium-entropy alloys at room temperature. *Tribol Int*. 2021;163:107160. <http://dx.doi.org/10.1016/j.triboint.2021.107160>.
6. Deevi SC. Advanced intermetallic iron aluminise coatings for high-temperature applications. *Prog Mater Sci*. 2021;118:100769. <http://dx.doi.org/10.1016/j.pmatsci.2020.100769>.
7. Rojacz H, Piringer G, Varga M. Iron aluminises: a step towards sustainable high-temperature wear resistant. *Mater*. 2023;523:204754.
8. Moghaddam AO, Fereidonnejad R, Cabot A. Semi-ordered high entropy materials: the case of high entropy intermetallic compounds. *J Alloys Compd*. 2023;960:170802. <http://dx.doi.org/10.1016/j.jallcom.2023.170802>.
9. Golovin IS. A Stella ic effects in Fe–Ga and Fe–Ga-Based alloys: a review. *Materials*. 2023;16(6):2365. <http://dx.doi.org/10.3390/ma16062365>.
10. Massalski TB, Murray JL, Bennett LH, Baker H. Binary alloy phase diagrams. *Metals Park: American Society for Metals*; 1986.
11. Liu Y, Yin F, Hu J, Li Z, Cheng S. Phase equilibria of Al–Fe–Sn ternary system. *Trans Nonferrous Met Soc China*. 2018;28(2):282-9. [http://dx.doi.org/10.1016/S1003-6326\(18\)64661-8](http://dx.doi.org/10.1016/S1003-6326(18)64661-8).
12. Alsaedi AK, Ivanova AG, Habieb AA, Almayahi BA. Show estimation of the functions of some iron-based ternary systems within Miedema model and comparison with experiment'. *Results Phys*. 2020;16:102969. <http://dx.doi.org/10.1016/j.rinp.2020.102969>.
13. Hojvat de Tendler R, Soriano MR, Pepe ME, Kovacs JA, Vicente EE, Alonso JA. Calculation of metastable free-energy diagrams and glass formation in the Mg–Cu–Y alloy and its boundary binaries using the Miedema model. *Intermetallics*. 2006;14(3):297-307. <http://dx.doi.org/10.1016/j.intermet.2005.06.008>.
14. Arzpeyma G, Gheribi AE, Medraj M. On the prediction of Gibbs free energy of mixing of binary liquid alloys. *J Chem Thermodyn*. 2013;57:82-91. <http://dx.doi.org/10.1016/j.jct.2012.07.020>.
15. Mousavi MS, Abbasi R, Kashani-Bozorg SF. A thermodynamic approach to predict formation enthalpies of ternary systems based on miedema's model. *Metall Mater Trans, A Phys Metall Mater Sci*. 2016;47(7):3761-70. <http://dx.doi.org/10.1007/s11661-016-3533-4>.
16. Jahangirim M. Investigation of the slipping wear based on the rate of entropy generation. *J Mod Processes in Manuf Prod*. 2014;3(1):47-57.
17. Nosonovsky M. Entropy in tribology: in the search for applications. *Entropy*. 2010;12(6):1345-90. <http://dx.doi.org/10.3390/e12061345>.
18. Lijesh KP, Khonsari MM. Characterization of multiple wear mechanisms through entropy. *Tribol Int*. 2020;152:106548. <http://dx.doi.org/10.1016/j.triboint.2020.106548>.
19. Biranvand KH, Vaezi M, Razavi M. Thermodynamic study of the formation of order-disorder structure of the nail intermetallic compound by semi-empirical model. *Physica B*. 2019;561:43-53. <http://dx.doi.org/10.1016/j.physb.2019.02.050>.
20. Alsaedi AK, Mraity HAA, Al-Temimei F. Application of Miedema's model for the calculation of thermodynamic properties of Fe–Al–Cr and Fe–Al–Cu ternary systems. *Res Square*. 2022. In press. <http://dx.doi.org/10.21203/rs.3.rs-2281016/v1>.
21. Zhang RF, Zhang SH, He ZJ, Jing J, Sheng SH. Miedema Calculator: a thermodynamic platform for predicting formation enthalpies of alloys within framework of Miedema's Theory. *Comput Phys Commun*. 2016;209:58-69. <http://dx.doi.org/10.1016/j.cpc.2016.08.013>.
22. Li H, Sun X, Zhang S. Calculation of thermodynamic properties of Cu–Ce binary alloy and precipitation behavior of Cu<sub>6</sub>Ce phase. *Mater Trans*. 2014;55(12):1816-9. <http://dx.doi.org/10.2320/matertrans.M2014319>.
23. Yelsukov EP, Ulyanov AL, Dorofeev GA. Comparative analysis of mechanisms and kinetics of mechanical alloying in Fe–Al and Fe–Si systems. *Acta Mater*. 2004;52(14):4251-7. <http://dx.doi.org/10.1016/j.actamat.2004.05.041>.
24. Voronina EV, Al'Saedi AK, Ivanova AG, Arzhnikov AK, Dulov EN. Structural and phase transformations occurring during the preparation of ordered ternary Fe–Al–M Alloys (with M = Ga, B, V, and Mn) by mechanical alloying. *Phys Met Metallogr*. 2019;120(12):1213-20. <http://dx.doi.org/10.1134/S0031918X19120172>.
25. Fu M, Ma X, Zhao K, Li X, Su D. High-entropy materials for energy-related applications. *iScience*. 2021;24(3):102177. <http://dx.doi.org/10.1016/j.isci.2021.102177>.
26. Wang R, Tang Y, Li S, Yuanlin AI, Li Y, Xiao B. Effect of lattice distortion on the diffusion behavior of high-entropy alloys. *J Alloys Compd*. 2020;825:154099. <http://dx.doi.org/10.1016/j.jallcom.2020.154099>.
27. Song O, Tian F, Hu Q-M, Vitos L, Wang Y, Shen J, et al. Local lattice distortion in high-entropy alloys. *Phys Rev Mater*. 2017;1(2):023404. <http://dx.doi.org/10.1103/PhysRevMaterials.1.023404>.